

F. Li  
 Jet Propulsion Laboratory  
 California Institute of Technology

### Introduction

This paper provides an overview of some recent developments in active microwave remote system systems at JPL. We describe the preliminary engineering and scientific results from the two recent flights of the Spaceborne Imaging Radar-C/X-band Synthetic Aperture Radar (SIR-C/X-SAR) on the space shuttle Endeavor. The key features of the radar design are summarized and the potential applications of the radar results to earth science are described. We also describe the recent progress in the development of interferometric SAR for high resolution topography mapping. The principle of this technique and results from airborne experiments are presented. Finally, development of meteorological radars for rain and cloud measurements is discussed. The design of an airborne rain mapping radar that was developed to support the Tropical Rainfall Measuring Mission is summarized. In addition, the design and development of an airborne 94 GHz cloud mapping radar are discussed.

#### 1. Spaceborne Imaging Radar-C/X-band Synthetic Aperture Radar (SIR-C/X-SAR)

SIR-C/X-SAR represents the third of a series of shuttle-borne imaging radars with increasing system capabilities and complexities. The SIR-C system operated at L- and C-band with quad-linear polarization measurement capability. It employed a phased array antenna with multiple transmit/receive (T/R) modules that are distributed across the antenna aperture. These multiple modules allow a graceful degradation in system performance in case of electronic part failures. The phased array design also allowed electronic beam steering which was used to acquire data at different antenna look angles. The X-SAR antenna was mechanically tilted to the same look angle when simultaneous measurements at all three frequencies were required. The details of the radar design and system performance characteristics can be found in Jordan et al [1]. The SIR-C system, with its multiple T/R modules, was designed to obtain fully polarimetric measurements with adequate signal-to-noise ratios for geophysical studies. Table 1 lists the key system parameters for SIR-C. In a subset of the radar operation modes, radar echoes were received simultaneously at the co- and cross-polarization channels. Upon signal processing on the ground, quad-linear polarization measurement for each of the pixels in the imagery were generated. Based on these polarization signature measurements, details of the mechanisms of the electromagnetic interactions of the radar signal and the terrain under study can be obtained (see Zebker and van Zyl [2]). Fig. 1 shows the SIR-C/X-SAR system within the shuttle bay during the mission. Fig. 2 shows the areas of the earth that were imaged during the two flights. Over 100 hours of radar data were collected in the two flights. Although the data collection were distributed across the globe, there was a concentration of data acquisition over a number of so-called supersites, in which extensive ground truth was also obtained for comparison with the radar results. This extensive data set from the SIR-C/X-SAR system is presently being analyzed for their applications in geology, ecology, hydrology and oceanography.

#### 2. Interferometric SAR

Digital topography data are a key input to a number of scientific, civilian and military applications. The available digital elevation model (DEM) data, however, have several significant limitations. For example, high resolution DEMs do not exist for many areas of the world. Even for the areas that have such DEMs, the Earth reference frame used

to generate the DEMs can be different and can lead to inconsistent data over the globe and conversion difficulties between data sets. A very promising technique to obtain a global, high resolution DEM with a consistent reference frame is interferometric synthetic aperture radar (IFSAR). This technique involves the flight of two SAR antennas that are separated by an interferometric baseline. Radar echoes received by the two antennas are then processed into two SAR images with the same spatial resolution of a conventional SAR. The two images are then coherently combined by subtracting the phase of a pixel from one image with the phase of the corresponding pixel from the other image. The resulting data, generally referred to as an interferogram, can be converted directly into the elevation of that pixel (see [3]). This technique is analogous to the conventional optical stereo technique, except that the parallax is measured by the phase difference, which is typically accurate to a small fraction of the SAR wavelength. The key significant advantages of this technique are that the radar can readily provide measurements of cloud-covered areas, the posting of the DEM derived is usually comparable to the inherent resolution of the SAR and, most importantly, the data processing can potentially be fully automated to allow a cost-effective, high throughput DEM production process.

We have implemented such an interferometric SAR system at C-band as part of the airborne SAR system that operates on the NASA Ames DC-8 (see [4]). Fig. 3 shows the SAR antennas that are mounted on the body of the DC-8 for this radar system. The two interferometric C-band antennas are separated by about 2 m. During the radar operation, radar signals are transmitted by one of these two antennas and the radar echoes received by both antennas are recorded separately onto high density tape recorders. The data are then subsequently processed into high resolution DEMs. An example of the elevation data obtained by this system of an area near Walnut Gulch, AZ, which had been converted to a perspective view, is shown in Fig. 4. We have developed detailed models relating the accuracy of the topography measurements to the radar system characteristics [5]. At present, evaluation of the actual accuracies of the data is underway. The initial assessment of the measurement accuracies is consistent with the system models. The results from this airborne system can now be routinely processed into digital topography data in a highly automated fashion. Given this progress, we have also been conducting studies of the feasibility of a spaceborne interferometric SAR mission for high resolution global topography mapping.

### 3. Airborne Rain and Cloud Mapping Radars

A key factor in our understanding of the global water and energy cycle is the accurate measurement of rainfall. As a step toward achieving this goal, the Tropical Rainfall Measuring Mission (TRMM) will be launched in the late 1990s to quantitatively measure the amount of rainfall in the tropics. It will carry as part of its payload a Precipitation Radar (PR). Rainfall measurement by radars on the ground remains a challenging problem because of the variations in the drop size distribution in space and time. Rainfall measurement by a spaceborne PR faces the same challenges and is further complicated by the downward-looking geometry and by the use of a high radar frequency because of the limitation in the antenna aperture that can be carried onboard a spacecraft and the desire to achieve the required spatial resolution. To support the TRMM PR, we have developed an airborne rain mapping radar (ARMAR) that also flies on the NASA Ames DC-8. It operates at 14 GHz, which is the same frequency as the TRMM PR. The downward-looking scanning geometry also mimics that of the TRMM PR. Fig. 5 and Table 2 show the observation geometry and the characteristics of ARMAR (see [61]). One key technological advance that we have implemented in this airborne radar is the use of a very low side-lobe pulse compression method. A traditional radar with restricted peak transmit power can improve the signal-to-noise ratio by using the pulse compression technique, in which a long duration, high bandwidth signal is transmitted. The received data are matched filtered by correlating them with a reference function, usually a replica of the transmitted signal with weighting. This technique has been applied to many spaceborne radars. However, the match filter processing typically creates pulse compression sidelobes. For a downward-looking rain radar, the ocean or ground return can be much stronger than the echoes from the raindrops. If a pulse compression technique is employed, the side-lobes of the surface return can significantly mask the return from the rain. In ARMAR, we have implemented a special pulse compression scheme that utilizes amplitude modulation of the transmitted pulse [7]. The resulting pulse compression sidelobes are typically below -55 dB. This low level is sufficient to prevent the contamination of the rain results by the surface return. ARMAR was successfully deployed during the TOGA/COARE experiment during January and February, 1993. More than 30 hours of tropical rainfall data were obtained. Analysis of the results are ongoing.

Finally, another radar system that is presently under development at JPL is an airborne cloud mapping radar. It is well recognized that clouds play a crucial role in the radiation budget of the earth. They modify the radiation reaching the Earth's surface, heat and cool different parts of the atmosphere directly, and they also indirectly affect the atmospheric energy balance through cloud-induced changes in water vapor. Despite the apparent abundance of space observations of clouds, the understanding derived from these observations is still hampered by the inability to resolve the vertical structure of clouds on a global basis. One promising remote sensing technique to provide such crucial measurements is a spaceborne millimeter wave cloud radar. Such a system has the potential of providing sufficient sensitivity and resolution for vertical structure measurements of most of the clouds of interest. To

develop a better understanding of the requirements for such a spaceborne radar and to collect the statistics of cloud characteristics, we are developing an airborne 94GHz cloud radar. At present, the detailed system requirements and interfaces have been identified and the subsystem design have been completed. The expected sensitivity of this system is extremely high and it should be able to detect and measure most of the clouds with significant impact on radiation balance. It is planned to be completed in the fall of 1996, and will be ready for scientific experiments in early 1997.

#### Acknowledgement

This work was performed at the Jet Propulsion Laboratory, California Institute of Technology, under contract with the National Aeronautics and Space Administration. I would like to acknowledge the efforts of the large team of Radar Scientists and Engineers who contributed to the results reported here.

#### Reference

1. "The SIR-C/X-SAR synthetic aperture radar system", Jordan, R., B. Huneycutt, and M. Werner, Proceedings of the IEEE, Vol. 79, no. 6, pp. 827-838, June 1991.
2. "Imaging Radar Polarimetry: A Review", Zebker, H., and J. Van Zyl, proceedings of the IEEE, vol 79, no. 11, pp. 1583-1607, November, 1991.
3. "Topographic Mapping from Interferometric Synthetic Aperture Radar Observations", Zebker, H., and R. Goldstein, J. Geophysical Research, Vol. 91, no. B5, pp. 4993-4999, 1986.
4. "The TOPSAR Interferometric Radar Topographic Mapping Instrument", Zebker, H., S. Madsen, J. Martin, K. Wheeler, T. Miller, Y. Lou, G. Alberti, S. Vetralla, and A. Cucci, IEEE Trans. Geoscience and Remote Sensing, vol. 30, no. 5, pp. 933-940, Sept, 1992.
5. "Studies of Multi-baseline Spaceborne Interferometric Synthetic Aperture Radars", Li, F., and R. Goldstein, IEEE Trans. Geoscience and Remote Sensing, vol. 28, no. 1, pp. 88-97, Jan 1990.
6. "ARMAR: An Airborne Rain Mapping Radar", Durden, S., E. Im, F. Li, W. Ricketts, A. Tanner, and W. Wilson, Journal of Atmos. and Oceanic Tech., Vol. 11, No. 3, pp. 727-737, June, 1994.
7. "Pulse Compression with Very Low Sidelobes in an Airborne Rain Mapping Radar", A. Tanner, S. Durden, R. Dennings, E. Im, F. Li, W. Ricketts, and W. Wilson, IEEE Trans. (Geoscience and Remote Sensing, Vol. 32, No. 1, pp. 211-213, Jan. 1994

**TABLE 11. SIR-C/X-SAR SYSTEM CHARACTERISTICS**

Parameter	L-band	C-band	X-band		
Orbital Altitude	225 Kilometers				
Wavelength	0.235 m	0.058 m	0.031 m		
Resolution	30 x 30 meters on the surface				
Swath Width	15 to 90 km	15 to 60 km			
Look Angle Range	20 to 55 Degrees from nadir				
Bandwidth	10 and 20 MHz				
Transmit Pulse Length	33, 17 and 8.5 usec	40 usec			
Pulse Repetition Rate	1240 to 1736 pulses per second				
Data Rate	90 Mbps	90Mbps	45 Mbps		
Data Format	8.4 bits/word & (8.4) BFPQ 4.6 bits/word				
Total Science Data	50 Hours/channel/mission				
Total Instrument Mass	11000 Kilograms				
DC Power Consumption	3000 to 7500 watts				

TABLE 2. ARMAR SYSTEM PARAMETERS.

Performance characteristics	
Range resolution (6-dB width)	50 m
Surface horizontal resolution (12-km altitude)	800 m
Swath width	9 km
Frequency	13.8 GHz
Polarizations	HH, VV, HV, VH
Antenna characteristics	
Aperture diameter	0.4 m
Gain	34 dB
3-dB beamwidth	3.8°
Sidelobe level	-32 dB
Polarization isolation	-28 dB
Transmitter characteristics	
Peak power	200 W
PRF	1-8 kHz
Number of transmit frequencies	1-4
Pulse duration	5-45 $\mu$ s
Chirp bandwidth	4 MHz
Receiver characteristics	
System noise temperature	650 K
Sample frequency	10 MHz
ADC resolution	12 bit
Radiometer characteristics	
Bandwidth	40 MHz
$\Delta T$ per pixel	1 K

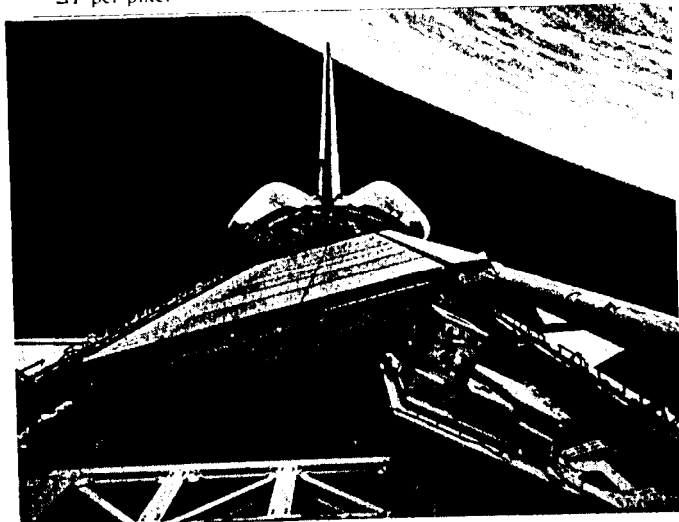


FIG 1.

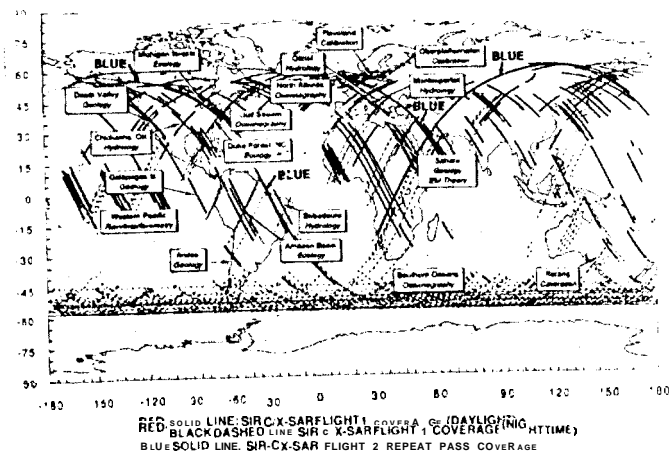


FIG 2.



FIG 3.

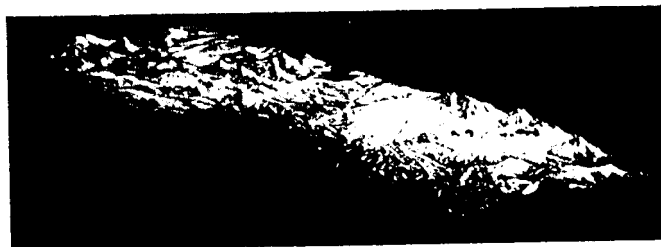


FIG 4.

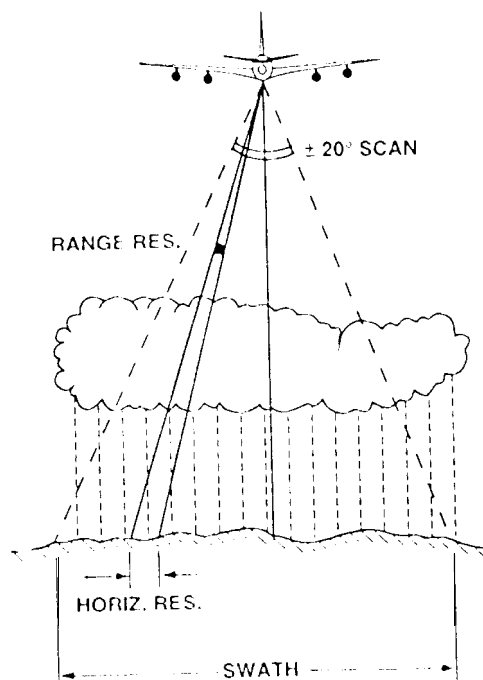


FIG 5. ARMAR OBSERVATIONAL GEOMETRY.